MAT JOURNALS

Journal of Alternative and Renewable Energy Sources
Volume 6 Issue 1

Heat Exchanger Analysis for Biomass-Powered Organic Rankine Cycle

James Bull[1], James M. Buick[2], Jovana Radulovic*[3]
[1]Ph.D Scholar, [2]Senior Lecturer, [3]Associate Head of School
School of Mechanical and Design Engineering, University of Portsmouth, UK

INFO

Corresponding Author:
E-mail Id:
**jovana.radulovic@port.ac.uk*

ABSTRACT

With ever-growing world energy demand, renewable and alternative energy solutions are more relevant than ever. Organic Rankine cycle (ORC) is a promising technology that offers a number of advantages over conventional power cycles. However, efficiency is relatively low and individual components can be costly. In this paper, we analysed performance of biomass-powered ORC that used benzene as a working fluid with the focus of the degree of superheat. Three superheated cycle scenarios, with max fluid temperature of 250°C, 300°C and 350°C, were considered. Energetic and energetic performances of three cycles were evaluated and heat exchanger sizing and analysis was carried out. While the overall power produced increases with the higher degree of superheat, the incremental improvement in efficiency requires a significantly larger heat transfer area. The optimal scenario offers a balance between efficiency, power output and the heat exchanger size.

Keywords: *Biomass, cycle, exchanger, organic rankine heat*

INTRODUCTION

Over the years, there has been increased focus towards renewable and sustainable energy sources as an alternative to finite fossil fuels in order to reduce global warming and address climate emergency. Research attention is directed towards improving technologies that efficiently utilise these energy sources. The Organic Rankine Cycle (ORC) is a power cycle, similar to the conventional Rankine Cycle, which uses organic working fluids as opposed to water to accommodate for low and medium temperature heat sources (< 400°C). Existing systems have been modelled and implemented in a variety of applications such as industrial/engine Waste heat recovery (WHR) [1], solar thermal plants [2, 3], biomass [4, 5] and geothermal sources [6].

The main components required for a simple ORC are a pump, evaporator, turbine and condenser. The working fluid is compressed by the pump to an increased pressure through the boiler to gain heat energy and evaporate to a vapour. Then, the vapour fluid expands through the

turbine to generate power returning to the initial pressure and finally condenses back to a liquid, expelling the remaining heat energy through the condenser to complete the cycle. Important factors that affect the performance of the cycle are the working fluid selection and the sources of heat loss within the system.

The working fluid selection is influenced by many aspects such as thermodynamic performance of the fluid, evaporation pressure and max cycle temperature [7]. In cycles with evaporation temperature less than 150°C, refrigerant fluids R113, R290 and R141b are often used. In cycles with higher temperatures (<250°C) it is more common to use aromatic hydrocarbons such as toluene or benzene. However, due to the vast differences in ORC objective functions, each cycle can have alternative optimal fluids. De Mena et al. [4] compared three working fluids for a higher temperature biomass heat source and identified that toluene demonstrated the best efficiency of 18.6% at an evaporating pressure and temperature of 25 bar and 300°C respectively. Toluene is a popular working fluid, thermodynamically outperforming benzene and cyclohexane across a range of pressures (5-20 bars) with an expander inlet temperature of 350°C. However, toluene requires a larger expansion device and as such, benzene is recommended as an alternative. Furthermore, benzene demonstrated increased stability when varying the expander inlet temperature.

For ORC systems with low-medium heat sources the electrical efficiency is often less than 20%, where the remainder of the energy is dissipated through system components, heat loss or rejected through the condenser [7, 8]. In some cases, the heat rejected through the condenser can be used for alternative purposes as proposed in combined heat and power plants (CHP) to increase the overall efficiency. However, this still does not account for all the energy losses. Previous research has identified that up to 90% of the exergy losses in the ORC system are due to the heat exchanger [9, 10]. In a study analysing the energy and exergy performance of different ORC setups, it was found that up to 70% of the exergy destruction in a simple ORC setup comes from the evaporator heat exchanger [11]. Furthermore, the costing of the heat exchanger contributes to a significant amount of the total ORC cost [12, 13]. Therefore, sizing and performance analysis of the heat exchanger is vital for the overall performance of an ORC system.

There are many different configurations of heat exchanger used for ORC systems. Commonly, fin and tube heat exchangers are used for WHR cycles within gas turbines or engines due to the increased surface area for the flues gases [14, 15]. Whereas, the compactness of plate heat exchangers enables significant advantages for systems with lower temperatures and pressures [16]. Shell and tube heat exchangers are often used for a variety of ORC applications such as geothermal power plants [17] and WHR systems [18]. Furthermore, shell and tube heat exchangers have simple geometries that can also be included in high pressure and temperature systems [19].

Xu et al. [20] compared the performance of shell and tube heat exchangers and plate heat exchangers for use in a subcritical ORC. The ORC used a simple setup with the working fluid R134a for an exhaust oil temperature of 120°C and upper and lower range pressures of 1.5-3MPa and 0.7-1MPa respectively. Overall, the shell and tube heat exchangers had higher thermal efficiency for the ORC and lower cost per kW. In comparison the plate heat exchangers has higher exergy efficiency and lower area per kW. These results indicate that a plate design is more

efficient for use in a smaller scale heat exchanger, whereas the shell and tube heat exchanger is cheaper and enables higher performance for the ORC system. This paper aims to investigate the performance of biomass-powered ORC with benzene as the working fluid. The effect of superheat and required heat transfer area is evaluated based on shell and tube heat exchanger model.

METHODOLOGY

The biomass-powered ORC is shown in Fig. 1. The stream of hot gas leaving the biomass combustor enters the heat exchanger at 400^{o}C. The condenser operating temperature was assumed to be 15^{o}C. Heat exchange was modelled as isobaric and no external heat losses were considered. Efficiency of the pump and the expander were 80% and 70%, respectively.

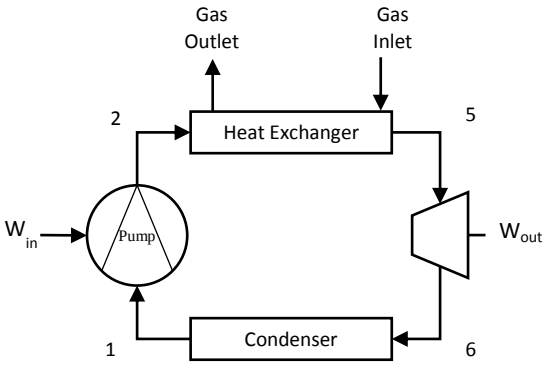

Figure 1: *ORC layout.*

REFPROP was used to determine relevant thermodynamic and transport properties, coupled with the following equations:

$$\eta_{Pump} = \frac{h_2 - h_1}{h_{2is} - h_1}$$

$$\eta_{Exp} = \frac{h_5 - h_6}{h_5 - h_{6is}}$$

$$W_{Net} = (h_5 - h_6) - (h_2 - h_1)$$

$$Q_{in} = h_5 - h_2$$

$$\eta = \frac{W_{Net}}{Q_{in}}$$

$$\dot{m}_{wf}(h_{out} - h_{in}) = \dot{m}_a c_{p,a}(T_{out} - T_{in})$$

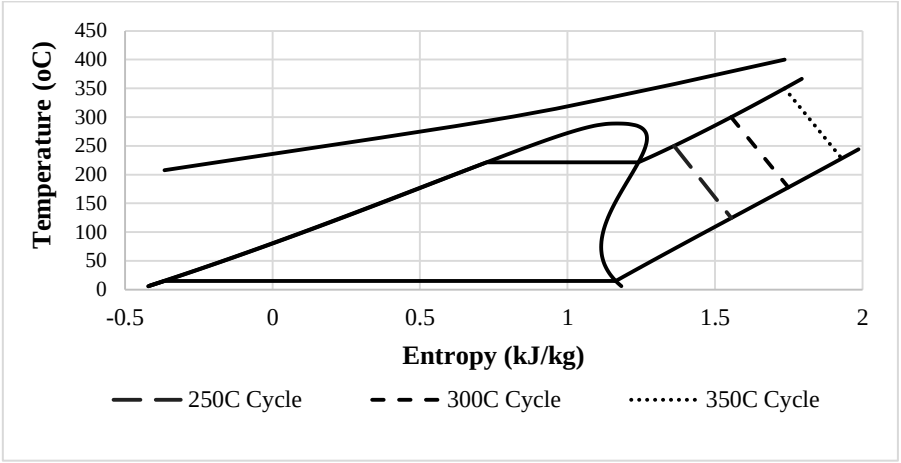

Figure 2: *T-s diagram of the three considered cycle scenarios.*

Fig. 2 T-s diagram of the three considered cycle scenarios: 250C (long dashed line), 300C (short dashed line) and 350C (dotted line). As a compromise between the cycle efficiency and safe operation, benzene pressure across the heat exchanger was assumed to be 20 bar. Given the saturated vapour temperature of benzene at 20 bar of 221.38°C, three different scenarios of the maximum temperature of the cycle (T_3) were considered: 250 °C, 300 °C and 350°C so evaluate the effect of superheat on the cycle performance and the required heat transfer area. This is demonstrated on the T-s diagram (Fig. 2). As benzene is a dry fluid, it is important to note the degree of temperatures at the outlet of the turbine due to the shape of the saturation curve. The exergy efficiency was evaluated using the following:

$$\eta_{ex} = \frac{W_{Net}}{Q_{in}\left(1 - \frac{T_0}{T_5}\right)}$$

with the exergy destruction for each component defined by:

Heat Exchanger

$$Ex_{dest,HE} = \dot{m}_{wf}\left((h_2 - T_0 s_2) - (h_5 - T_0 s_5)\right) + \dot{m}_{wf}(h_5 - h_2)\left(1 - \frac{T_0}{T_5}\right)$$

Expander:

$$Ex_{dest,Exp} = \dot{m}_{wf}\left((h_5 - T_0 s_5) - (h_6 - T_0 s_6)\right) + \dot{m}_{wf}(h_5 - h_6)$$

Condenser:

$$Ex_{dest,Cond} = \dot{m}_{wf}\left((h_6 - T_0 s_6) - (h_1 - T_0 s_1)\right)$$

Pump:

$$Ex_{dest,Pump} = \dot{m}_{wf}\left((h_1 - T_0 s_1) - (h_2 - T_0 s_2)\right) + \dot{m}_{wf}(h_2 - h_1)$$

In this paper shell and tube heat exchanger configuration was selected with the internal tube containing the working fluid (benzene) in a shell of the exhaust gas. To account for the phase change of the working fluid, the heat exchanger calculations were split in three sections: pre-heater, evaporator and super heater. Tube thickness was assumed to be negligible and no fouling as considered. For each section, average thermal properties were used.

Table 1: *Design Parameter.*

Design Parameter	Value
Gas Mass Flow Rate	0.38 kg/s
Benzene Mass Flow Rate	0.08 kg/s
Diameter of Tube, d_T	0.01m
Diameter of Shell, d_s	0.06m
Number of Tubes	1
Number of Shells	1
Number of Tube Passes	2

The heat transfer area required was evaluated using LMTD method:

$$A = \frac{Q_{ht}}{U\Delta T_{LM}}$$

$$\Delta T_{LMCF} = \frac{\Delta T_1 - \Delta T_2}{\ln\left(\frac{\Delta T_1}{\Delta T_2}\right)}$$

with correction factor (F) incorporated for the pre-heater and super-heater sections:

$$F = \frac{\sqrt{R^2+1}}{(R-1)} \frac{\ln\left(\frac{1-P}{1-PR}\right)}{\ln\left(\frac{\frac{2}{P} - 1 - R + \sqrt{R^2+1}}{\frac{2}{P} - 1 - R - \sqrt{R^2+1}}\right)}$$

$$\Delta T_{LM} = \Delta T_{MCF} F$$

The overall heat transfer coefficient was determined as:

$$U = \frac{1}{\frac{1}{h_{wf}} + \frac{1}{h_{tf}}}$$

where the heat transfer coefficient for the working fluid side and the thermal fluid side are given by:

$$h = \frac{Nu \cdot k}{D}$$

The values for the Nusselt number were calculated using the well-known Dittus-Boelter correlation:

$$Nu = 0.023 Re^{0.8} Pr^{0.4}$$

The Shah correlation for two-phase flow was additionally incorporated for the heat transfer coefficient in the phase change section:

$$h_{lv} = h_l \left[(1-x)^{0.8} + \frac{3.8 x^{0.76} (1-x)^{0.04}}{p_r^{0.38}} \right]$$

Where *x* is the mixture quality and the reduced pressure was calculated as:

$$p_r = \frac{p_{crit}}{P_2}$$

RESULTS

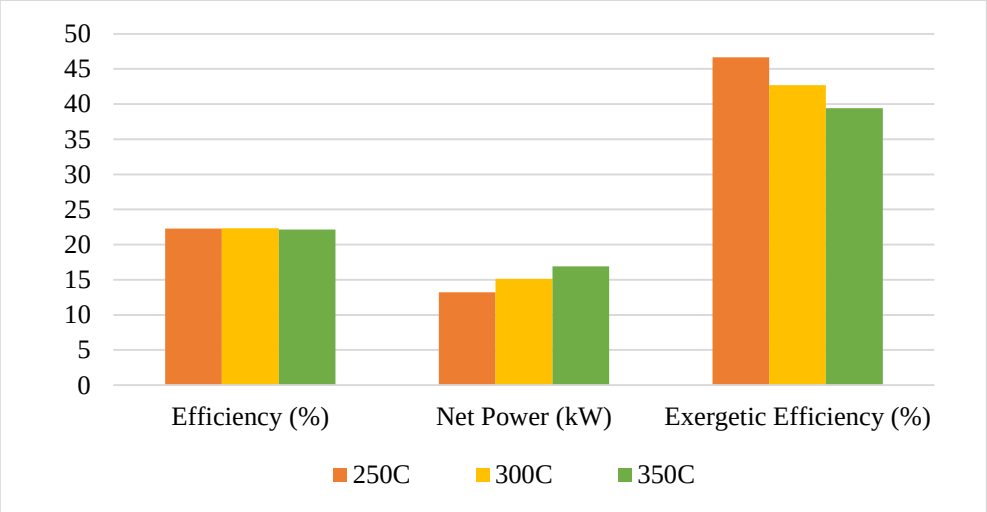

Figure 3: *ORC Performance: thermal efficiency, net power and energetic efficiency.*

The main performance characteristics evaluated for the three considered max temperatures are presented in Fig. 3. The net power produced increases with the maximum cycle temperature due to the larger heat input to the evaporator. The efficiency demonstrated minimal difference across the 250, 300 and 350 cycles, varying by only 0.2%. Comparing the results to Mena (2017), benzene had higher efficiency by at least 3.5% across all three cycles whilst operating at a lower pressure. Interestingly, the energy efficiency decreases as the maximum temperature of the cycle increases, indicating the 250°C cycle utilises the heat available in the most efficient manner. As shown in Fig. 3, the pump has a negligible impact on the overall exergy destruction. Furthermore, the corresponding exergy destruction during the expansion process for the 250, 300 and 350 cycles were

calculated as 4.239 kW, 4.237 kW and 4.228 kW respectively, showing minimal difference with respect to the maximum temperature change. In all cases the evaporator and condenser contributed to the largest percentage of exergy destruction (71.6, 78.9 and 83.5, respectively) in line the trend reported elsewhere (Chen et al., 2012; Quoilin et al., 2011). As maximum cycle temperature increases, the exergy destruction within the evaporator and condenser also increase. Alternative ORC setups such as turbine bleeding or a regeneration cycle could be employed to utilise more exergy within the evaporator process.

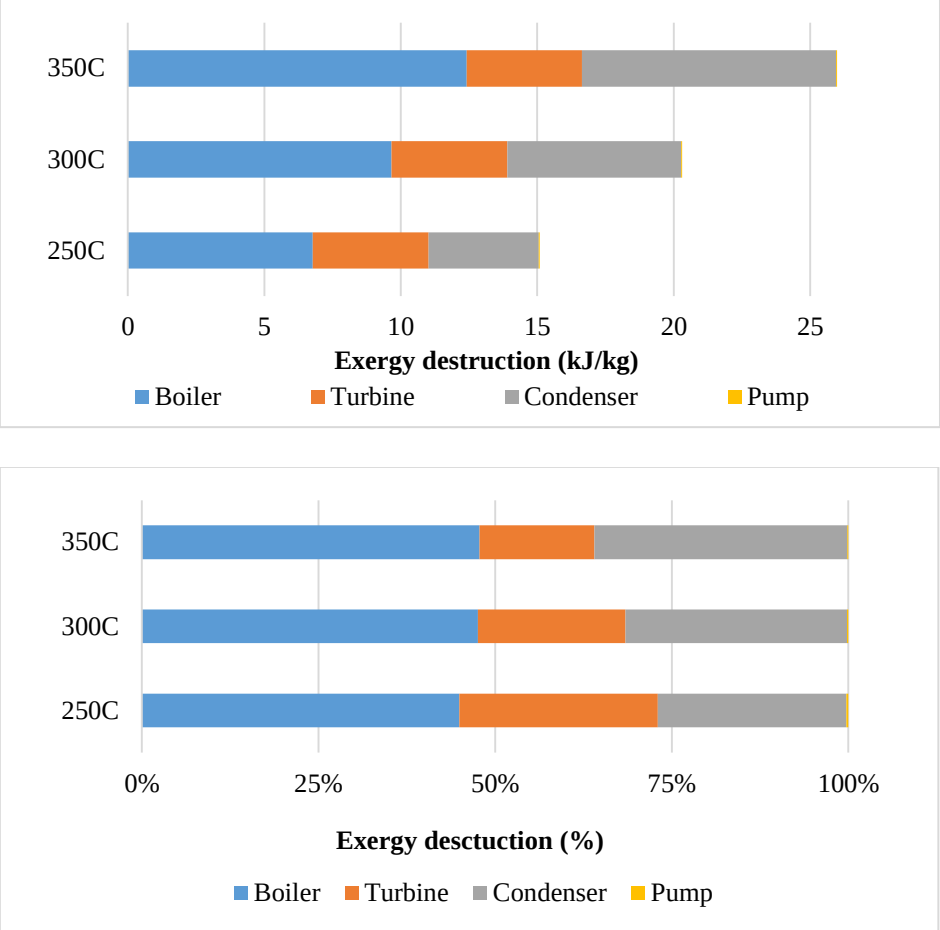

Figure 4: *Exergy destruction in individual ORC components.*

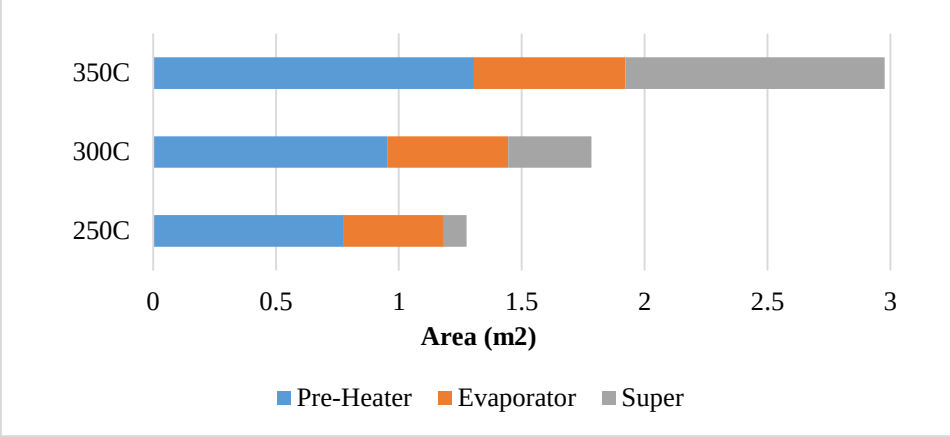

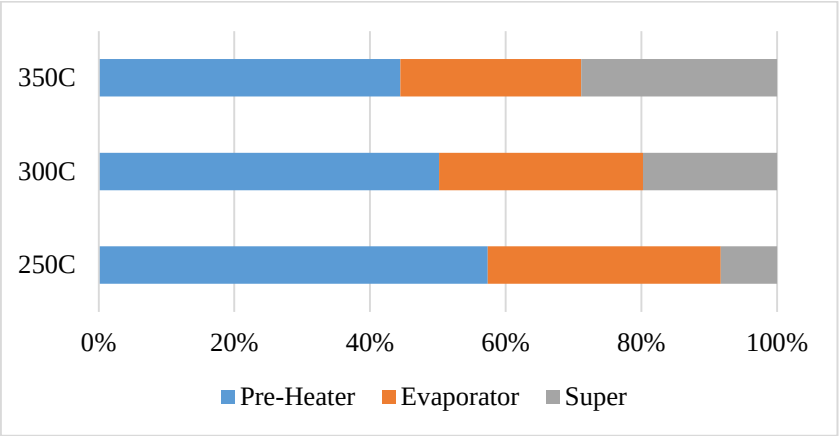

Figure 5: *Heat transfer area and percentage of heat transferred per section.*

The exergy destruction in the condenser can be related to the fluid temperature at the expander. As benzene is a dry fluid, the shape of the saturation curve affects the phase change point for superheated vapour at lower pressures. Subsequently, this causes the temperature at the outlet of the expander to be higher compared to wet or isentropic fluids, and as a result increases the exergy destruction in the condenser shown in 4.

Heat transfer area required for each section of the ORC in shown in Fig 5. Remarkably, the 250 cycle has an overall heat transfer area ($1.267m^2$) smaller than the preheater section for the 350 cycle ($1.306m^2$). In fact, with the current system setup the 250 cycle heat transfer area is less than half of the 350 cycle at $2.977m^2$.

Fig. 5 also depicts the percentage of heat transferred per section. In all three cases the pre-heater section required the greatest amount of heat transferred. For the 250 and 300 cycles, the smallest percentage of heat transferred is required for fluid super heating 8.3% and 19.8%, respectively. However, in the 350 cycle the phase change section contributes the smallest percentage of heat transferred at 26.6%, which is 2.24% less than the super heating section.

Fig. 6, Demonstrates the exergy destruction per section within the heat exchanger. Overall, the exergy destruction within the heat exchanger decreases as the maximum temperature increases. However, for the superheat section the exergy destruction increases with maximum temperature due to the additional heat transfer required to meet the higher temperature needs.

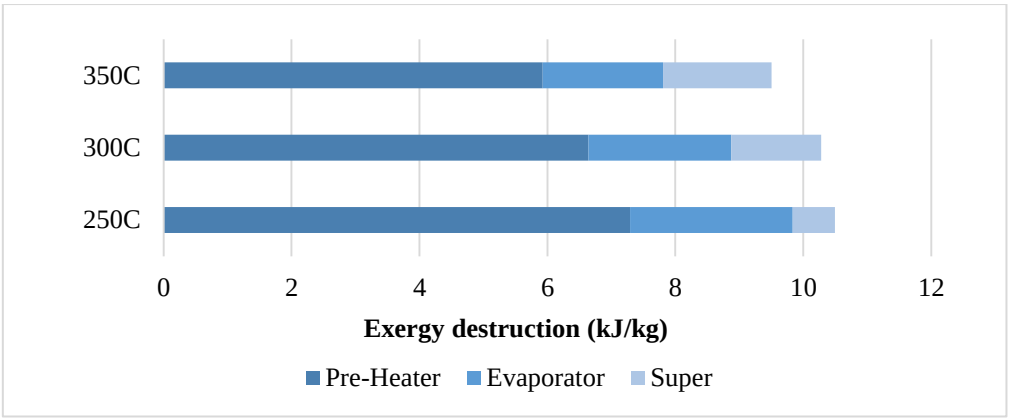

Figure 2: *Exergy destruction per section of the heat exchanger.*

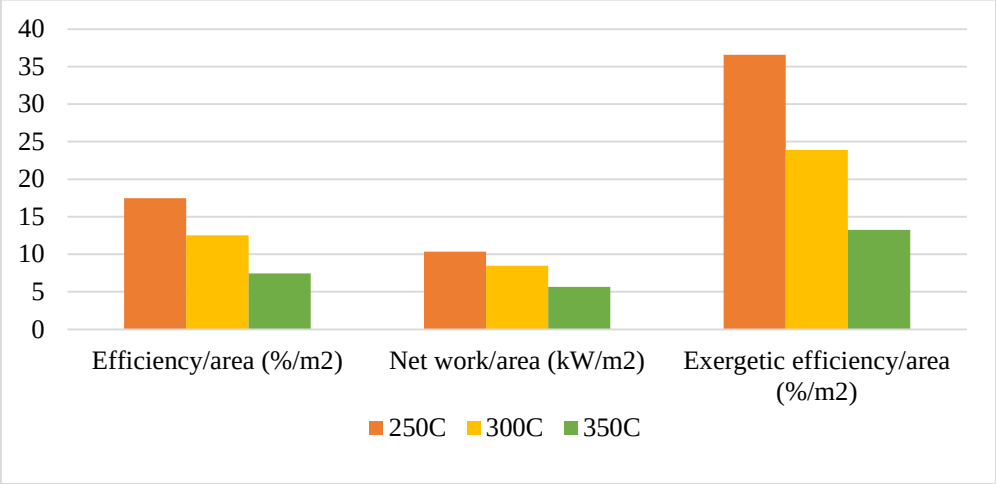

Figure 3: *ORC performance relative to the required heat transfer area.*

Taking the performance of each ORC cycle in relation to heat exchanger design into consideration,

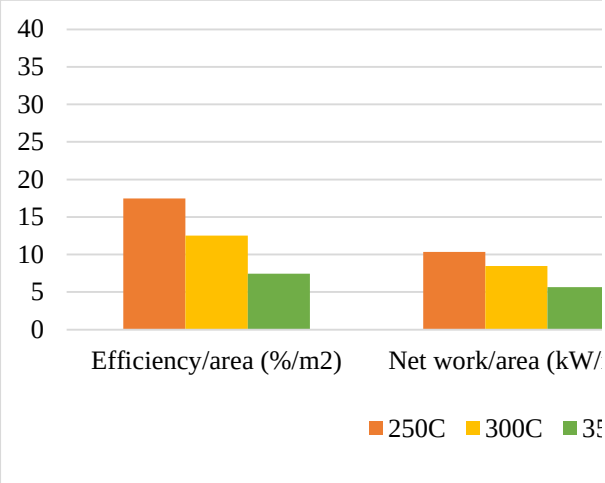

Figure ***3*** indicates that the 250 cycle has the most efficient use of area per characteristic observed. As maximum cycle temperature increases, this efficiency decreases. Although, when comparing to previous literature the heat exchangers modelled within this paper all demonstrated lower heat exchanger area per network, than both shell, tube and plate heat exchangers for a lower maximum cycle temperature (Xu et al., 2015). This may be due to the difference in the initial ORC and heat exchanger parameters selected. Nonetheless, further study should be conducted to see if the observed differences in plate and shell and tube heat exchangers are comparable to an ORC of similar setup to that used within this paper.

CONCLUSIONS

Performance of a simple biomass-powered ORC was been evaluated in three different scenarios by adjusting the max temperature of the superheated working fluid between 250-350C.

Our results indicate that the lowest degree of superheat (250C) requires smaller heat transfer area than the other two and yields the highest exergy efficiency.

On the other hand, higher degree of superheat increases the new work achieved. The exergy destruction was found to be the lowest for the heat exchanger in 350C scenario. However, 350 scenario requires a heat exchanger twice the size of 250 one.

REFERENCES

1. Scaccabarozzi R, Tavano M, Invernizzi C M, et al. (2018), “Comparison of working fluids and cycle optimization for heat recovery ORCs from large internal combustion engines”, *Energy*, Volume 158, Issue 1, pp. 396–416, https://doi.org/10.1016/j.energy.2018.06.017.
2. Kumar A., Shukla S. K (2016), “Analysis and performance of ORC based solar thermal power plant using benzene as a working fluid”, *Procedia Technology*,

Volume 23, pp. 454–463, https://doi.org/10.1016/j.protcy.2016.03.050.
3. Zhang Y, Deng S, Zhao L, et al. (2017), "Clarifying the bifurcation point on Design: A Comparative Analysis between Solar-ORC and ORC-based Solar-CCHP", *Energy Procedia*, Volume 142, pp. 1119–1126, https://doi.org/10.1016/j.egypro.2017.12.365.
4. De Mena B, Vera D, Jurado F, et al (2017), "Updraft gasifier and ORC system for high ash content biomass: A modelling and simulation study", *Fuel Processing Technology*, Volume 156, pp. 394–406, https://doi.org/10.1016/j.fuproc.2016.09.031.
5. Kalina J, Swierzewski M, Szega M, (2017), "Simulation based performance evaluation of biomass fired cogeneration plant with ORC", *Energy Procedia*, Volume 129, pp. 660–667, https://doi.org/10.1016/j.egypro.2017.09.137.
6. Bianchi M, Branchini L, De Pascale A, et al, (2018), "Performance and operation of micro-ORC energy system using geothermal heat source", *Energy Procedia*, Volume 148, pp. 384–391, https://doi.org/10.1016/j.egypro.2018.08.099.
7. Quoilin S, Van Den Broek M, Declaye S, et al, (2013), "Techno-economic survey of Organic Rankine Cycle (ORC) systems", *Renewable and Sustainable Energy Reviews*, Volume 22, pp. 168–186, https://doi.org/10.1016/j.rser.2013.01.028.
8. Schuster A, Karellas S, Kakaras E, et al. (2009), "Energetic and economic investigation of Organic Rankine Cycle applications", *Applied Thermal Engineering*, Volume 29, Issue 8–9, pp. 1809–1817, https://doi.org/10.1016/j.applthermaleng.2008.08.016.
9. Chen Q, Xu J, Chen H. (2012), "A new design method for Organic Rankine Cycles with constraint of inlet and outlet heat carrier fluid temperatures coupling with the heat source", *Applied Energy*, Volume 98, pp. 562–573, DOI: https://doi.org/10.1016/j.apenergy.2012.04. 035.
10. Quoilin S, Declaye S, Tchanche B F, et al. (2011), "Thermo-economic optimization of waste heat recovery Organic Rankin Cycles", *Applied Thermal Engineering*, Volume 31, Issue 14–15, pp. 2885–2893, DOI: https://doi.org/10.1016/j.applthermaleng.2011.05.014.
11. Safarian S, Aramoun F. (2015), "Energy and exergy assessments of modified Organic Rankine Cycles (ORCs)", *Energy Reports*, Volume 1, pp. 1–7, DOI: https://doi.org/10.1016/j.egyr.2014.10.003.
12. Lecompte S, Huisseune H., Van Den Broek M, et al. (2013), "Part load based thermo-economic optimization of the Organic Rankine Cycle (ORC) applied to a combined heat and power (CHP) system", *Applied Energy*, Volume 111, pp. 871–881, DOI: https://doi.org/10.1016/j.apenergy.2013.06.043.
13. Walraven D, Laenen B, D'haeseleer W. (2014), "Comparison of shell-and-tube with plate heat exchangers for the use in low-temperature organic Rankine cycles", *Energy Conversion and Management*, Volume 87, pp. 227–237, DOI: https://doi.org/10.1016/j.enconman.2014.07.019.
14. Jung H C, Krumdieck S, Vranjes T. (2014), "Feasibility assessment of refinery waste heat-to-power conversion using an organic Rankine cycle", *Energy Conversion and Management*, Volume 77, pp. 396–407, DOI: https://doi.org/10.1016/j.enconman.2013.09.057.
15. Kaya A, Lazova M, De Paepe M. (2015), "Design and rating of an evaporator for waste heat recovery organic rankine cycles using SES36", *3rd International Seminar on ORC Power Systems*, Presented at the ASME 2015 International Mechanical Engineering Congress and Exposition, Brussels, Belgium, Paper ID: 192, pp. 1–10.
16. Imran M, Usman M, Park B S, et al.

(2015), "Multi-objective optimization of evaporator of organic Rankine cycle (ORC) for low temperature geothermal heat source", *Applied Thermal Engineering*, Volume 80, pp. 1–9, DOI: org/10.1016/j.applthermaleng.2015.01.034.

17. Nigusse H A, Ndiritu H M, Kiplimo R. (2014), "Performance Assessment of a Shell Tube Evaporator for a Model Organic Rankine Cycle for Use in Geothermal Power Plant", *Journal of Power and Energy Engineering*, Volume 2, pp. 9–18, DOI: https://doi.org/10.4236/jpee.2014.210002.
18. Liu L, Pan Y, Zhu T, et al. (2017), "Numerical predicting the dynamic behavior of heat exchangers for a small-scale Organic Rankine Cycle", *Energy Procedia*, Volume 129, pp. 419–426, DOI: https://doi.org/10.1016/j.egypro.2017.09.127.
19. Towler G, Sinnott R. (2012), "Chemical Engineering Design: Principles, Practice and Economics of Plant and Process Design", (2nd edition), *Elsevier Science and Technology*, Volume 6, pp. 1-15.
20. Xu J, Luo X, Chen Y, et al. (2015), "Multi-criteria design optimization and screening of heat exchangers for a subcritical ORC", *Energy Procedia*, Volume 75, pp. 1639–1645, DOI: https://doi.org/10.1016/j.egypro.2015.07.397.